The Inhibitory Effects of ACD-crosslinked Actin Oligomers on mDia1 Mediated Actin Polymerization

A Senior Honors Thesis

Presented in partial fulfillment of the requirements for graduation *with research distinction* in Biochemistry in the undergraduate colleges of The Ohio State University

By

Dmitry Grinevich

The Ohio State University

April 2014

Project Advisor: Dr. Dmitri Kudryashov, Department of Chemistry and Biochemistry

Table of Contents

Abbreviations

- G-actin: Monomeric actin
- F-actin: Filamentous actin
- ABP: Actin binding protein
- hPro1: Human profilin 1
- mDia1: Mouse diaphanous related formin 1
- MARTX: Multifunction autoprocessing repeats in-toxin
- ACD: Actin crosslinking domain
- V_c: *Vibrio cholera*
- A_h: *Aeromonas hydrophila*
- FH1/2: Formin homology 1/2
- MBP: Maltose binding protein
- FA: Fluorescence anisotropy

Acknowledgements

I have been a part of the Kudryashov lab at the Ohio State University Biochemistry/Chemistry department for approximately one year. Dr. Kudryashov has been a great scientific mentor for the time I have spent working with him and has given me great amounts of knowledge not only in biochemistry, but how to conduct research and work in a lab in general. He has taught me not only how to work and learn efficiently, but also how to write about my work and then present it to others. For all of his patience and effort that he has made in teaching me, I would like to thank him. I would also like to thank Kudryashov lab members Elena Kudryashova and David Heisler for further teaching me and providing endless help and advice when needed. Third, I would like to thank all other members of the Kudryashov lab with whom I have worked with in the past for their support and contribution to the highly enjoyable lab research experience. Lastly, I would like to thank The Ohio State University's Department of Chemistry and Biochemistry for financial assistance with the award of the URS scholarship and for the funding of my research, making this work possible.

Abstract

The actin crosslinking domain (ACD) is an actin-specific toxin produced as a part of larger toxins by pathogenic Gram-negative bacteria *Vibrio cholerae, Vibrio vulnificus,* and *Aeromonas hydrophila*. When the toxin is delivered to the cell, ACD catalyzes the crosslinking of actin monomers into non-polymerizable actin oligomers of varying size. The current view is that the crosslinked oligomers have a passive role in damaging the cytoskeleton, i.e. that ACD activity disrupts the actin cytoskeleton due to a gradual accumulation of non-functional actin oligomers which leads to depletion of both the monomeric and filamentous actin pools. Due to the effectiveness of the toxin at low cellular concentrations, it is possible that the oligomers have a more active role in the disruption of the cytoskeleton.

Actin oligomers exhibit a unique combination of properties, different from G- and F-actin, giving them the ability to interact with G-actin binding proteins while possessing tandem binding sites. We hypothesized that ACD-crosslinked oligomers should have a higher affinity for tandem actin-profilin binding proteins. Specifically, the ability of the formin homology 1 (FH1) domain of formins to bind profilin-actin complexes could be interrupted by these crosslinked actin oligomers. We tested this hypothesis by exploring the interactions of these actin oligomers with the mouse formin mDia1. The method used in order to study protein activity is pyrene-labeled actin polymerization assay. We found that nanomolar concentrations of actin oligomers, when preincubated with profilin, inhibited mDia1-mediated polymerization in a concentration dependent manner. This project elucidates a novel, unexplored toxicity mechanism implemented by ACD to affect actin dynamics, leading ultimately to cell rounding and cell death.

Characterization of this inhibition highlights the striking efficiency of bacterial toxins and the ways in which they can hijack cellular machinery to accomplish their goals.

1. Introduction

Actin is a highly conserved structural protein found in nearly all eukaryotic cells. Actin is found in primarily two forms, filamentous (F-actin) and monomeric (G-actin), which exhibit distinct functional properties. Dynamic assembly of G-actin into F-actin filaments is important for numerous cellular functions including, but not limited to cell division, cell motility, and endo- and exocytosis (Schoenenberger et al., 2011). Monomeric actin has 4 subdomains, with 1 and 3 being structurally similar and most likely arisen from gene duplication. Subdomains 2 and 4 are also similar to each other and appear to be large insertions into subdomains 1 and 3 (Figure 1) (Dominguez and Holmes, 2011). The subdomains are arranged to form two binding clefts. The cleft between subdomains 2 and 4 is responsible for nucleotide binding (ATP or ADP) and binding of a related cation (typically Mg^{2+}) (Figure 1). The cleft between subdomains 1 and 3 is lined by primarily hydrophobic residues and is involved in binding to several important regulators of actin dynamics – thymosin β4, cofilin, profilin, twinfilin, gelsolin, and other proteins (Dominguez and Holmes, 2011). G-actin can spontaneously polymerize into helical filaments (F-actin) under physiological conditions *in vitro* (Pollard and Cooper, 2009). Polymerization of filaments, along with formation of new filaments, is tightly regulated through the hydrolysis of ATP and the interaction with numerous actin binding proteins (ABP), including Arp2/3 complex proteins and formins, which are a focus of this study. Once a pre-existing filament is present, polymerization occurs very rapidly (Pollard and Cooper, 2009), unless filament ends are blocked (capped) with specific capping proteins. Actin filaments polymerize

faster at the barbed end (+), and at steady state conditions they will depolymerize at the pointed end (-) which allows for directional growth of filaments necessary for motility. In innate immunity, these actin functions are translated into chasing bacterial cells by macrophages and neutrophils, and eliminating pathogenic bacteria via secretion of humoral factors (e.g. antibodies, proteases, defense peptides, etc.) and by phagocytosis (Netea et al., 2012). The functional versatility of actin makes it an appealing target for bacterial toxins, allowing pathogens to undermine numerous vital functions of actin or hijack the actin cytoskeleton for their own benefits (Kudryashov et al., 2008a).

Our studies focus on the actin crosslinking domain (ACD) - an actin-specific effector domain within the larger MARTX and VgrG1 toxins found in pathogenic Gram-negative bacteria *Vibrio cholerae*, *Vibrio vulnificus*, and *Aeromonas hydrophila* (Satchell, 2009). These bacteria are diarrheal pathogens which secrete enterotoxins to colonize the host intestines (Kudryashov et al., 2008a). Both toxins are known to induce rapid cell rounding in cell cultures due to the disassembly of filamentous actin (Satchell, 2009). MARTX toxins disrupt the cytoskeleton by two mechanisms: 1) the Rho-GTPase inhibitory domain (RID) shifts the cell's actin equilibrium towards monomeric actin by adversely affecting actin cytoskeleton regulation by a family of small GTPases (Rho, Rac, Cdc42) (Kudryashov et al., 2008b). 2) ACD catalyzes the formation of an isopeptide bond between the K50 and E270 residues of two or more actin monomers, resulting in the formation of polymerization incompetent dimers, trimers, and higher order oligomers (Figure 2) (Cordero et al., 2006). As ACD crosslinks cellular actin monomers, this leads to the depolymerization of actin stress fibers causing cell rounding and eventually leading to cell death in severe cases . The activity of ACD is dependent on the normal cellular co-factors

ATP and Mg^{2+}, but does not require the presence of other toxin domains or other host cell proteins (Cordero et al., 2006). The isopeptide bond formed during crosslinking exists between actin residues K50 and E270 which are located within the most flexible loops of actin (Kudryashov et al., 2008b). Both of these loops are unstructured and protrude from the body of the actin monomer. The crosslink brings together lysine and glutamine residues, whose alpha carbons are normally separated by a distance of 17 to 25 Å in actin filaments (Kudryashov et al., 2008b). Therefore, the crosslinking disrupts the typical arrangement of actin protomers as they would exist in a filament which compromises their ability to participate in normal cellular functions. Because of this, the ACD-crosslinked actin oligomers do not polymerize.

The current view of ACD pathogenesis is that these crosslinked actin oligomers have a passive role in disrupting the actin cytoskeleton due to a gradual accumulation of non-functional actin oligomers and the depletion of both monomeric and filamentous actin pools (Figure 5) (Satchell, 2009). In contrast, we predict that the actual mechanisms by which ACD shuts down cellular functions of actin are more efficient, so that only a few copies of the toxin delivered to the cytoplasm of a host cell would suffice to adversely affect cellular actin dynamics.

We propose that the actin oligomers actively affect normal interactions of actin with ABPs, and therefore the toxin can act at substantially lower doses and neutralize host immune cells faster than is currently recognized. We suggest that the structural difference between the ACD-crosslinked actin oligomers and both G- and F-actin translates into altered interactions of the actin oligomers with actin binding proteins. Actin oligomers exhibit the unique ability to

bind G-actin proteins, while at the same time possess multiple binding sites (a property of F-actin). Particularly, we propose that due to a tandem organization, the ACD-crosslinked actin oligomers should have a substantially higher affinity to tandem actin binding proteins. To test this hypothesis, we focused on possible interactions between formins and crosslinked actin oligomers.

The focus of this thesis project is on the impact of ACD crosslinked actin oligomers on formin-mediated actin polymerization, specifically the mouse formin mDia1. Formins are an important type of ABP involved for the formation of filopodia, polarized cell growth, and cytokinetic rings (Breitsprecher and Goode, 2013). Formins are a diverse class of proteins characterized by common formin homology domains but varying in functions and domain arrangement. The functional part of formin proteins consists of two domains known as formin homology domains I and II (FH1 and FH2), which are important for actin nucleation and elongation, respectively. FH2 is a highly structured domain composed of primarily alpha helices, which form a donut-shaped homodimer (Paul and Pollard, 2009). The lasso region at the N-terminus of FH2 can bind to the post region at the C-terminus of the next subunit in order to stabilize the dimer. The FH2-FH2 dimer interacts with the barbed end of actin filaments and remains processively associated with the growing filament, efficiently blocking filament capping proteins (Figure 3) (Paul and Pollard, 2009). As new actin monomers are attached to the filaments, the FH2 dimer is able to move along with the growing filament end. Typically, actin filaments with FH2 bound at the end grow more slowly than free actin filaments, implying that FH2 works by a gating mechanism where it has open and closed conformations which either allow or prevent the addition of actin monomers, respectively (Paul and Pollard, 2009). It is

proposed that these changing conformations are responsible for the processive movement along the filament. The other important role of the FH2 domain is the stabilization of actin nuclei, a process known as nucleation. Nucleation of a new filament is the rate limiting step of actin polymerization as it requires 3 actin monomers to form the initial stable nucleus needed for the filament to grow. Once a nucleus of actin monomers or pre-existing filament is present, polymerization occurs very rapidly. The FH2 dimer assists in reducing the energetic cost of creating these nuclei and promotes their formation.

While the FH2 dimer mediates nucleation and assists in attachment to the actin filament, the acceleration of filament elongation is performed by the FH1 domains located at the N-termini of the FH2 domains, resulting in two FH1 domains for each dimer. FH1 is believed to be an intrinsically unstructured domain containing tandem tracks of repeating proline residues (known as poly-proline rich regions). It is important to note that cellular G-actin exists in a complex with a sequestering protein, either profilin or thymosin β (Dominguez and Holmes, 2011). Profilin binds to actin monomers at the barbed face (between subdomains I and III) preventing spontaneous nucleation of actin filaments (Bugyi and Carlier, 2010). The opposite side of profilin binds to poly-proline sequences, allowing profilin-actin complexes to interact with the poly-proline tracks of FH1 domains (Figure 4A).

Because a majority of monomeric actin is in the profilin-actin complex, the interaction between profilin and formins is extremely relevant (Paul and Pollard, 2009). It is known that in the presence of low concentrations of profilin, FH1-FH2 domains of formins accelerate barbed end polymerization. The mechanism by which profilin-actin works together with formins to

accelerate polymerization is not explicitly known. However, it has been shown that poly-proline regions are able to bind profilin-actin complexes with varying affinities; the further the poly-proline rich region is from the growing filament end, the higher the affinity (Courtemanche and Pollard, 2012). The accepted mechanism suggests that formins accelerate the rate of polymerization by increasing the local concentration of actin near the barbed end (Figure 4A) (Paul and Pollard, 2009). This allows for actin monomers to be quickly incorporated into the filament as they are brought to the barbed end with the aid of the flexible FH1 arms.

The reason we chose to focus on formins in the context of the ACD toxin is because they possess the FH1 domain which has tandem actin-profilin binding sites. Specifically, we hypothesized that this tandem arrangement will allow for significantly stronger interactions between actin oligomers and FH1 than lone profilin-actin complexes. The regions connected by the covalent bond in actin oligomers are located away from the profilin binding site in the hydrophobic cleft of actin and profilin does not inhibit the crosslinking reaction (Figure 5). This allows for the actin oligomers to bind profilin and therefore interact with the poly-proline regions in FH1 domains of formins. If properly spaced, the complexes of profilin and the crosslinked oligomers would bind to FH1 domains of formins with great affinity due to the avidity of multiple binding sites allowing for stronger interactions. Ultimately, the goal of this project is to test the formulated hypothesis and study the effects of ACD-crosslinked actin oligomers on mDia1-mediated polymerization *in vitro* using bulk pyrene-actin polymerization assay. If interactions are occurring between the profilin-bound actin oligomers and mDia1, the polymerization-accelerating function of mDia1 should be altered.

2. Results and Discussion

2.1 Optimization of mDia1 purification and storage conditions

Preparation of the C-terminal fragment of mDia1 (MBP-FH1-FH2-6xHis-tag) was started by transformation of pET21A vector into *E. Coli* and overexpression; this vector was received as a gift from Dr. David Kovar (University of Chicago). The protein contains a maltose binding protein (MBP) domain and a 6xHis-tag allowing for either amylase resin or immobilized metal affinity chromatography (IMAC) purification, respectively (Figure 6). We were able to increase protein yield by making improvements to the bacterial overexpression protocol. Sequence analysis, using a ProtParam program (ExPASy), revealed that mDia1 contains 130 total prolines, located primarily within the FH1 domain poly-proline tracks (Gasteiger et al.). Therefore, we supplemented our growth medium with 0.5 mM of free L-proline during protein expression (Figure 7). We speculate that the addition of free proline reduces the stress on the cells to produce proline for protein synthesis and ultimately results in a better yield of mDia1. Conventional expression conditions followed by initial IMAC purifications yielded approximately 0.84 mg protein/L of media, while supplementation with free L-proline resulted in a near four fold increase (3.3 mg protein/L of media) in yield (Figure 7).

It has been previously reported that mDia1 cannot be frozen following purification without a significant loss of activity (Moseley et al., 2006). Therefore, we explored methods that would allow for long term storage of mDia1. We explored the storage conditions by supplementing mDia1 with 50% glycerol or 50% ethylene glycol and freezing at -20 °C, or leaving mDia1 at 4 °C. After 2 weeks, all samples were tested for their efficiency of actin nucleation and elongation (Figure 8). The highest retained activity was from the sample stored

at -20 °C in 50% glycerol; this condition was used routinely to preserve to purified protein for subsequent experiments.

2.2 Profilin purification and isoform selection

As a class of proteins, profilins are specialized in regulating actin polymerization, but also have the ability to interact with repeating sequences of proline residues, known as poly-proline tracks. This allows for various isoforms of profilin to be purified using highly specific type of column chromatography. Free poly-L-proline can be attached to Sepharose resin in order to make a chromatography column which will specifically bind to profilins. This allows for the binding of any profilin isoform on this column under native conditions and elution with increasing concentrations of denaturants. After purification using the poly-L-proline column, profilin can be further cleaned up with fast protein liquid chromatography (FPLC) to remove high molecular weight contaminants. Refolding of human profilin I was carried out by repetitive dialysis changes into storage buffer which lacks the denaturant. It was also important to determine which species-specific form of profilin would be optimal to use with mDia1. We purified and tested profilin from *Mus musculus, Saccharomyces pombe,* and *Homo sapiens* using the poly-L-proline column, and tested the effect on mDia1-mediated polymerization. Our results showed that mDia1 functioned best with human profilin (hPro1), so this isoform was selected for our experiments.

2.3 Actin-oligomer formation by ACD

The reproducible formation of actin oligomers by ACD was a critical step for generating consistent results. Due to ACD being able to crosslink any free actin monomers, active ACD must either be removed or inactivated after the formation of actin oligomers. Initially a 6xHis-

tagged ACD from *Vibrio cholera* (ACD_{Vc}) was used, removal of which was attempted by mixing the reaction with TALON cobalt resin. This method resulted in some loss of actin oligomers through non-specific binding to the resin. Moreover, it was observed that this method did not completely remove ACD_{Vc} from our reactions. Actin crosslinking occurring in our bulk pyrene-actin polymerization assays was evident on an SDS-PAGE gel confirming the presence of active ACD (Figure 9). The concentrations of oligomers used in this polymerization assay were in the nanomolar range, therefore they cannot be visualized by SDS-PAGE, meaning new additional oligomers were being formed by active toxin. This control shows that even residual amounts of ACD were able to cause significant crosslinking of pyrene-labeled actin, thus producing artificial results. To resolve this issue, we used an ortholog from *Aeromonas hydrophila* (ACD_{Ah}), a psycroptrophic, gram negative bacteria. Our lab has shown that $ACD_{Ah,}$, when heated to 42 °C, is unfolded and deactivated. Using ACD_{Ah} removed the need for using IMAC purification, since thermal treatment ultimately eliminated any ACD activity. Following heat inactivation of ACD_{Ah}, stability and lifetime of actin oligomers on ice was improved by supplementation with 1 mM of ATP. Inactivation by heat showed to be efficient and reliable, allowing us to successfully synthesize fully functional actin oligomers that were free of active ACD_{Ah}.

2.4 Effects of actin oligomers on mDia1-mediated polymerization, observed by bulk pyrene-actin polymerization assay

Pyrene-actin bulk polymerization assay is an effective method of observing bulk actin polymerization rates *in vitro.* It allows for a measurement of actin polymerization rates by observing the increase in fluorescent signal emitted by pyrene-actin as it is incorporated into filaments. It has been shown that the fluorescent signal is independent of filament length

distribution, and that pyrene-actin and regular actin exhibit the same time course of polymerization, elongation rate constants, intrinsic viscosity, and critical concentration (Cooper et al., 1983). This allows for an overall view of how quickly monomeric actin is being incorporated into filaments, with the rate being proportional to the increase in fluorescent signal. This assay is highly sensitive and is optimal for studying actin polymerization *in vitro,* because it does not interfere with regular actin filament dynamics.

Under normal cellular conditions, mDia1 greatly increases actin filament polymerization rates in the presence of profilin. We hypothesized that actin oligomers, which can also bind profilin, may be able to also occupy these tandem sites and inhibit mDia1 mediated polymerization. As controls, we first compared the rates of actin polymerization and mDia1 accelerated polymerization in the presence and absence of nanomolar concentrations of actin oligomers, with no profilin present. Because the tandem-binding sites of mDia1 possess poly-proline tracks, the binding of actin-profilin complexes depends on the ability of profilin to bind actin and then also bind to the poly-proline regions. In this situation, the actin oligomers should have no way of binding to or interfering with mDia1. The addition of actin oligomers to either system did not affect actin polymerization rates, meaning our controls verified that the interaction requires profilin, and that actin oligomers on their own do not affect the dynamics of this system (Figure 10).

Next, in order to test our hypothesis, we introduced human profilin into the system and observed how varying concentrations of actin oligomers affected polymerization. While holding actin and profilin concentrations at 2.5 uM and 5 uM, respectively, and mDia1 in a low nanomolar range (between 1 and 10 nM), we varied the concentrations of actin oligomers from

200 pM to 10 nM. At concentrations of actin oligomers that exceed the amount of mDia1 present, we found that polymerization was completely inhibited. Using varying concentrations of actin oligomers below the concentration of mDia1 showed a dose-dependent inhibition (Figure 11). In the experiment depicted in Figure 11, a concentration of 5 nM mDia1 was used, along with concentrations of oligomers ranging from 1-10 nM. Next, we used our titration data to make an estimate of the binding affinity between actin oligomers and the FH1 domain. This value was determined by fitting the inhibition seen by actin oligomers on elongation rates to an isothermal binding curve (Figure 12). Data for curve was collected by observing the time it takes for the reaction to reach half the value of the polymerization plateau. At this halfway point, the slope was measured to give a value for the rate of the reaction at those conditions. By plotting a relative rate of elongation versus the concentration of actin oligomers, we found an apparent K_D in the sub-nanomolar range (0.089 nM, Figure 12) of the actin oligomers for the mDia1 FH1 domains. This value for K_D is not exact because the experiment involves using a mixed population of actin oligomers, varying in size. Varying sized actin oligomers will have different affinities, meaning our mixed sample will give us an overall average of all different actin oligomers, making it an apparent estimate for the whole population. This strong binding affinity confirms our hypothesis that the tandem binding sites of actin oligomers allow for significantly stronger interactions with FH1 than lone profilin-actin complexes.

Because the inhibitory effect of the actin oligomers on mDia1 was not observed in the absence of profilin, the inhibition is profilin-dependent. The only way that profilin interacts with mDia1 is through the tandem poly-proline regions of the FH1 domain, implying that the profilin-bound actin oligomers bind to these regions via profilin interactions. Our data show that the

actin oligomers actually have an even stronger affinity for these sites than profilin-actin complexes because the actin oligomers can bind to multiple sites at the same time. Once bound, the actin oligomers are able to block the FH1 domain and prevent it from bringing in new actin-profilin complexes for filament elongation, ultimately shutting down the elongation activity of mDia1.

Our data indicate that the actin oligomers have functionality and effects on other cellular proteins, not previously known in the field of ACD-containing toxins. This means that the damage caused to cells by ACD is more complex than just the depletion of free actin and a shutdown of cells by disassembly of the actin cytoskeleton. Bacterial toxins have evolved to function at maximum efficiency, using the crosslinked actin oligomers produced by the toxin as tools to interfere with functions of other cellular proteins. The inhibitory effects shown here demonstrate how highly efficient bacterial pathogens can be and how they are able to greatly affect vital cellular functions with only a small amount of toxin and/or crosslinked actin.

The significance of this project is multifaceted. First, the project provides a novel insight into the mechanism of the host immune system subversion by pathogenic bacteria. Second, studying the ACD-containing MARTX and VgrG1 toxins, produced by *Vibrio cholera* and other human pathogens, provides an understanding of their pathogenic pathways which can help in facilitating their efficient elimination. Finally, formins have not previously been identified as targets of bacterial toxins. This highlights the fact that our understanding of how these toxins carry out their function is still not fully complete and their mechanisms are more complicated than previously believed. The understanding of the detailed role of the ACD-crosslinked actin

oligomers should allow us to create tools to ultimately study and control formin mediated processes.

3. Future Directions

3.1 Cloning and expression of FH1 for fluorescence anisotropy

To evaluate the affinity of profilin-bound actin oligomers for the poly-proline tracks, we attempted to clone and purify only the FH1 domain of mDia1. Initially, we used polymerase chain reaction (PCR), with primers designed to amplify the sequence coding only the FH1 domain of mDia1. The PCR product was cloned into pCold-TEV using the In-Fusion cloning system (Clontech, Mountain View, CA). In-Fusion uses the vacinnia virus DNA polymerase (VVpol) which takes advantage of complementary strands between the vector and the PCR product to perform single-strand annealing that fuses the PCR product with the vector (Irwin et al., 2012). However, we were not able to successively purify FH1 following overexpression. This was confirmed through MALDI, which showed that the molecular weights of the pure species did not match with the predicted molecular weight of the FH1 domain. FH1 domains are highly disordered regions and may be easily degraded by proteases or be insoluble upon expression. To overcome these issues, we recently have attempted to increase the stability/solubility of FH1 by fusion with MBP at the N-terminus of FH1 (MBP-FH1) Once expressed and purified, FH1 can be labeled with the amine-reactive fluorescent probe Atto610 to determine the binding affinities of actin oligomers to mDia1 FH1 domains using fluorescence anisotropy assays (Park and Raines). FA quantifies changes in polarization (which is a function of size/tumbling rate) of a fluorescently-labeled protein due to its interaction with other, preferably larger, molecules. Therefore, the affinity of FH1 domains for actin oligomers of different sizes in the presence of

profilin will be measured by detecting changes in anisotropy of the Atto610 probe bound to the FH1 domain. Understanding the strength of this binding will give significant insight into the strength of this interaction and inhibitory effect.

3.2 Cloning and expression of FH2-FH1FH2 heterodimer

To further study the inhibitory effect of actin oligomers on mDia1, and differentiate whether the effect occurs by binding to a single FH1 arm, cross-two arm, or a mixed binding of actin oligomers, we produced a "single-armed" mDia1, consisting of two FH1 domains and one FH1 domain (Figure 4C). Due to the high affinity of FH2 domains for each other, we expect that co-expression of a FH1-FH2 and a FH2 domain, with different tags, will allow for isolation of the heterodimeric protein (Courtemanche and Pollard, 2012). For the coexpression, the pETDuet-1 vector was chosen because it possesses two separate multiple cloning sites (MCS) with both under the control of the T7 promoter, allowing for the co-expression of two proteins. To allow for the purification of the heterodimer, two different affinity tags would need to be present in the sequence. First, we inserted MBP-FH1-FH2 into MCS1, followed by insertion of FH2-6xHis into MCS2. This order of insertions was vital because the restriction enzymes used for the first cloning event (NcoI and HindIII) would also have digested part of the FH2 sequence had the order been reversed. The set of restriction enzymes used for the second cloning event (NdeI and XhoI) could be safely used as they did not cut outside of MCS2. Following sequencing verification that both inserts where correct, the resulting plasmid was transformed into BL21(DE3)-pLysS expression cells.

We optimized the expression of the heterodimer by testing it under varying conditions. Initially, ten different colonies were screened on a small scale using varying temperatures (16,

25, and 37 °C), concentrations of ITPG (0.5, 1, and 2 mM), and the length of expression (2.5, 4, 8, and 16 hours). The best expression was found from expression at 37 °C overnight induced with 1 mM IPTG (Figure 13). Using this clone, expression was carried out in 2 L of growth medium under the identified optimal conditions. Isolation of the heterodimer required a tandem purification set up that would allow us to separate it from two homodimers. First, IMAC purification would allow for the removal of the MBP-FH1-HF2 homodimer, because it does not contain a 6xHis tag. Following elution with imidazole from IMAC column, the eluted fractions containing proteins need to be buffer exchanged by dialysis into amylase-column binding buffer prior to MBP-purification. This will result in the separation of the 6x His-tagged FH2-FH2 homodimer (in the flow through) and the heterodimer (bound to the resin). Following elution with 10 mM maltose, the heterodimer will be dialyzed into formin storage buffer A (see methods). Once successfully expressed and purified, this heterodimer can be used in the same bulk pyrene polymerization assays to further study the mechanism of observed actin-oligomer inhibition. This protein is currently in the process of being tested but no results are available at the time of this document.

4. Materials and Methods

This chapter outlines and describes the protocols used to prepare and carry out the experiments described previously. Preparation of acetone powder of rabbit muscle, monomeric actin preparation, and cloning for FH1 and FH2-FH1FH2 heterodimer was done in collaboration with graduate student David Heisler. Preparation of pyrene labeled actin was done by David Heisler. Actin was prepared from rabbit muscle acetone powder (Pardee and Spudich, 1982).

After extraction from the acetone powder, fresh G-actin was prepared by dialysis overnight against a G-buffer: 2 mM Tris-HCl pH 8, 0.2 mM CaCl2, and 0.2 mM ATP.

4.1 MBP-FH1-FH2-6xHis purification

To prepare MBP-FH1-FH2-6xHis (C-terminus of mDia1), we transformed pET21A vector encoding the sequence of interest into BL21 Codon Plus *E. coli* under ampicillin and chloramphenicol resistance. Cell cultures were grown up to OD_{600}=1.2 in MMI media (1.25% tryptone, 2.5% Sigma yeast extract, 125 mM NaCl, 0.4% glycerol, 50 mM Tris pH=8.2) before induction. mDia1 expression was initiated with addition of 1 mM IPTG and 0.5 mM L-proline and was continued for 6 hours at 25 ˚C. Cells were pelleted at 3000 *xg* for 20 min at 4 C. Pellets were then resuspended in buffer A (50 mM NaH_2PO_4, 500 mM NaCl, 10% glycerol, 10 mM imidazole, pH=8.0) supplemented with protease inhibitors (2 ug/mL Leupeptin/Pepstatin, 2 ug/mL Trypsin inhibitor) and then freeze-thawed using liquid nitrogen three times to activate lysozyme to break down cell walls. The cell lysate was sonicated twice under the following conditions: 60% amplitude, 6 second pulse, 1 second off, 2 minutes sonication. Next, the lysate was clarified by centrifugation at 20,000 rpm for 20 min at 4 ˚C. The supernatant was then filtered through a Whatman filter and supplemented with 0.1 mM PMSF. This lysate was nutated with Talon cobalt resin beads (Clontech) for 1 hour and then loaded onto a column. The resin was washed with 50 mL of buffer A, then washed with 15 mL of buffer A supplemented with 20 mM imidazole, and finally the protein was eluted in 1.5 mL fractions by using buffer A supplemented with 250 mM imidazole. The content of each fraction was analyzed by SDS-PAGE and samples with purified protein were pooled, concentrated, and

dialyzed into storage buffer for later use (20 mM Tris pH=8.5, 50 mM NaCl, 5% glycerol, 0.01% NaN_3).

4.2 ACD purification

To prepare His-LF_N-ACD_{Vc}, we transformed pCold vector encoding the sequence of interest into BL21 DE3 P-Lys *E. coli* under ampicillin and chloramphenicol resistance. Cell cultures were grown up to OD_{600}=1.2 in MMI media before induction. His-LF_N-ACD_{Vc} expression was initiated with addition of 1 mM IPTG and was continued for 16 hours at 15 ˚C. After expression, cells were pelleted at 3000 *xg* for 20 min at 4 ˚C. Pellets were then resuspended in buffer B (20 mM Tris, 500 mM NaCl, 2 mM $MgCl_2$, 10 mM imidazole, 0.5 mM PMSF, pH=8.0) supplemented with protease inhibitors (2 ug/mL Leupeptin/Pepstatin, 2 ug/mL Trypsin inhibitor) and then freeze-thawed using liquid nitrogen three times to activate lysozyme to break down cell walls. The cell lysate was sonicated twice under the following conditions: 60% amplitude, 6 second pulse, 1 second off, 2 minutes sonication. Next, the lysate was clarified by centrifugation at 20,000 rpm for 20 min at 4 ˚C. The supernatant was then filtered through a Whatman filter and supplemented with 0.1 mM PMSF. This lysate was nutated with Talon cobalt resin beads (Clontech) for 1 hour and then loaded onto a column. The resin was washed with 80 mL of buffer B, then washed with 15 mL of buffer B supplemented with 20 mM imidazole, then washed with 15 mL of buffer B supplemented with 50 mM imidazole, and finally the protein was eluted in 1.5 mL fractions using buffer B supplemented with 250 mM imidazole. The content of each fraction was analyzed by SDS-PAGE and samples with minimal contamination were pooled, concentrated, and dialyzed for later usage (20 mM Tris pH=8.5, 50 mM NaCl, 5% glycerol, 0.01% NaN_3).

4.3 Human profilin purification

To prepare hPro1, we transformed pMW vector encoding the sequence of interest into BL21 DE3 P-Lys *E. coli* carrying ampicillin and chloramphenicol resistance. Cell cultures were grown up to OD_{600}=1.2 in MMI media before induction. hPro1 expression was initiated with addition of 1 mM IPTG and was continued for 4 hours at 37 ˚C. After expression, cells were pelleted at 3000 *xg* for 20 min at 4 ˚C. Pellets were then resuspended in buffer C (10 mM Tris, 150 mM NaCl, 1 mM EDTA, 1 mM DTT, pH=8.0) supplemented with protease inhibitors (2 ug/mL Leupeptin/Pepstatin, 2 ug/mL Trypsin inhibitor) and then freeze-thawed using liquid nitrogen three times to activate lysozyme to break down cell walls. The cell lysate was sonicated twice under the following conditions: 60% amplitude, 6 second pulse, 1 second off, 2 minutes sonication. Next, the lysate was clarified by centrifugation at 20,000 rpm for 20 min at 4 ˚C. The supernatant was then filtered through a Whatman filter and supplemented with 0.1 mM PMSF. This lysate was nutated with poly-L-proline resin for 1 hour and then loaded onto a column. The resin was washed with 100 mL of buffer C, then washed with 50 mL of buffer C supplemented with 1 M Urea, and finally the protein was eluted in 1.5 mL fractions using buffer C supplemented with 3 M Urea. The content of each fraction was analyzed by SDS-PAGE and samples with purified protein were pooled, concentrated, and dialyzed for later usage (2 mM Tris pH=8.0, 0.2 mM EGTA, 1 mM DTT, 0.01% NaN_3).

4.4 Actin crosslinking by ACD

The ACD crosslinking reaction was carried out by crosslinking 20 uM of skeletal actin with 10 nM of ACD_{Ah} in oligomer reaction buffer (10 mM Tris pH=8.0, 0.1 mM PMSF, 200 uM ATP). Actin was diluted from an initial 100 uM stock containing 0.2 mM Ca^{2+}. All components

except $MgCl_2$ were combined and equilibrated to the same temperature by storage on ice, and then the reaction was initiated with addition of 1 mM $MgCl_2$. After initiation, the reaction was ran at 10 C for 15 minutes, then heated to 42 ˚C for 10 minutes and supplemented with additional 2 mM $MgCl_2$. Additional $MgCl_2$ was added to polymerize any actin that had not been crosslinked once ACD was inactivated by heat. Next, this reaction was chilled on ice for 5 minutes and then held at room temperature for 15 minutes before centrifuging at 90,000 rpm for 30 minutes at 4 ˚C to separate actin oligomers from actin filaments. The resulting supernatant was supplemented with 1 mM ATP and kept on ice for storage and use in experiments.

4.5 Bulk pyrene-actin polymerization assays

Bulk pyrene-actin polymerization assays were set up by pre-incubating all of our proteins of interest before initiation of the polymerization reaction with $MgCl_2$. Formin reaction buffer (10 mM MOPS pH=7.0, 0.2 mM ATP, 0.5 mM DTT) was combined with 2.5 uM pyrene actin (5% labeled), and depending on the specific sample, also combined with hProf1 (5 uM), mDia1 (1-10 nM), or actin oligomers (0.2-10 nM). Samples were loaded into a 384 well plate and fluorescence was measured by excitation at 366 nM and reading emission at 407 nM. Next, calcium ions were chelated using switch buffer (10 mM MOPS pH=7.0, 0.2 mM ATP, 0.5 mM DTT, 0.3 mM EGTA, 0.1 mM $MgCl_2$) and fluorescence was measured for another 2 minutes. The reaction was initiated with initiation buffer (10 mM MOPS pH=7.0, 0.2 mM ATP, 0.5 mM DTT, 1

mM $MgCl_2$) and fluorescence was measured until polymerization was complete. Changes in fluorescence were measured for 4 hours with time points taken every 30 seconds.

4.6 PCR and cloning of recombinant proteins

PCR for making recombinant MBP-FH1 was run in 1x Phusion GC buffer (New England Biolabs), combined with 200 uM dNTPs, 500 nM of both forward and reverse primers, 10 ng of MBP-FH1-FH2-6xHis plasmid (KV373) as a template, and 6% ethylene glycol. 1 unit of Phusion polymerase (New England Biolabs) was added to initiate the PCR reaction. Initial denaturation was ran for 30 seconds at 98 C. The PCR was then run for 30 cycles with a denaturation step (10 seconds, 98 ˚C), an annealing step (30 seconds, 55-72 ˚C), and an extension step (30 seconds, 72 ˚C). The PCR product was confirmed to be the correct size by agarose gel electrophoresis and then purified from the gel. This PCR product was transformed into pColdTEV, a modified expression vector containing a protease cleavage site, using the Clontech InFusion kit. The InFusion reaction was run by combining digested pColdTEV with MBP-FH1 PCR product and the InFusion polymerase and the reaction was performed at 50 ˚C for 15 minutes. The product of the InFusion reaction was transformed into DH5α competent cells, purified and confirmed by sequencing.

PCR and cloning reactions for the heterodimer constructs were performed using the same reagents with appropriate plasmids and primers for heterodimer sequences. Two PCR products were made: one containing the sequence of FH2-6xHis, and one containing the sequence of MBP-FH1-FH2. First, we inserted MBP-FH1-FH2 into the first multiple cloning site of pETDuet by InFusion. Next, FH2-6xHis was inserted into the second multiple cloning site by

InFusion. InFusion reaction conditions in both cloning events were 50 ˚C for 15 minutes. In each InFusion reaction, the cut plasmid was prepared by digesting pETDuet with NcoIII and HindIII for multiple cloning site 1 and Nde1 and Xho1 for multiple cloning site 2. Following sequencing verification, the resulting plasmid will be transformed into BL21(DE3)-pLysS expression cells for determination of optimal expression conditions.

6. Figures

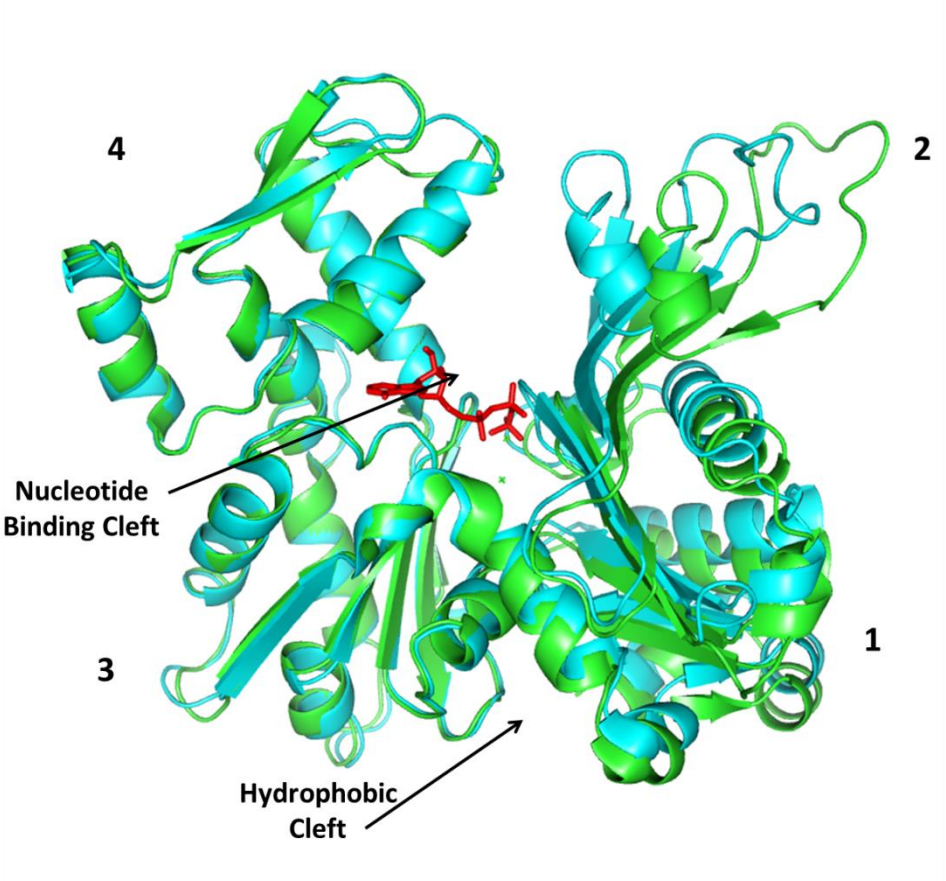

PDB: 1HLU, 2BTU

Figure 1. X-ray crystal structure of an actin monomer. This structure shows an actin monomer in its open (green) and closed (blue) states. The 4 subdomains are labeled by number and the nucleotide binding cleft is bound with ATP (red). The hydrophobic cleft binds to G-actin binding proteins, including profilin.

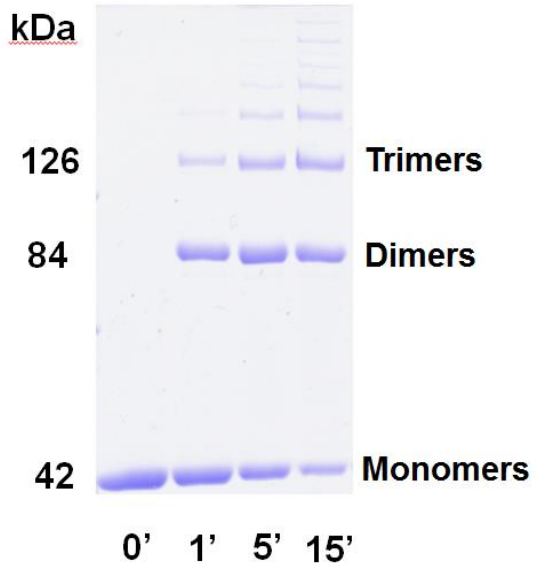

Figure 2. Time course of ACD activity. Significant crosslinking of actin monomers occurs within the first 15 minutes of combining active ACD with actin at room temperature. Formation of many higher order structures is observed within this time frame.

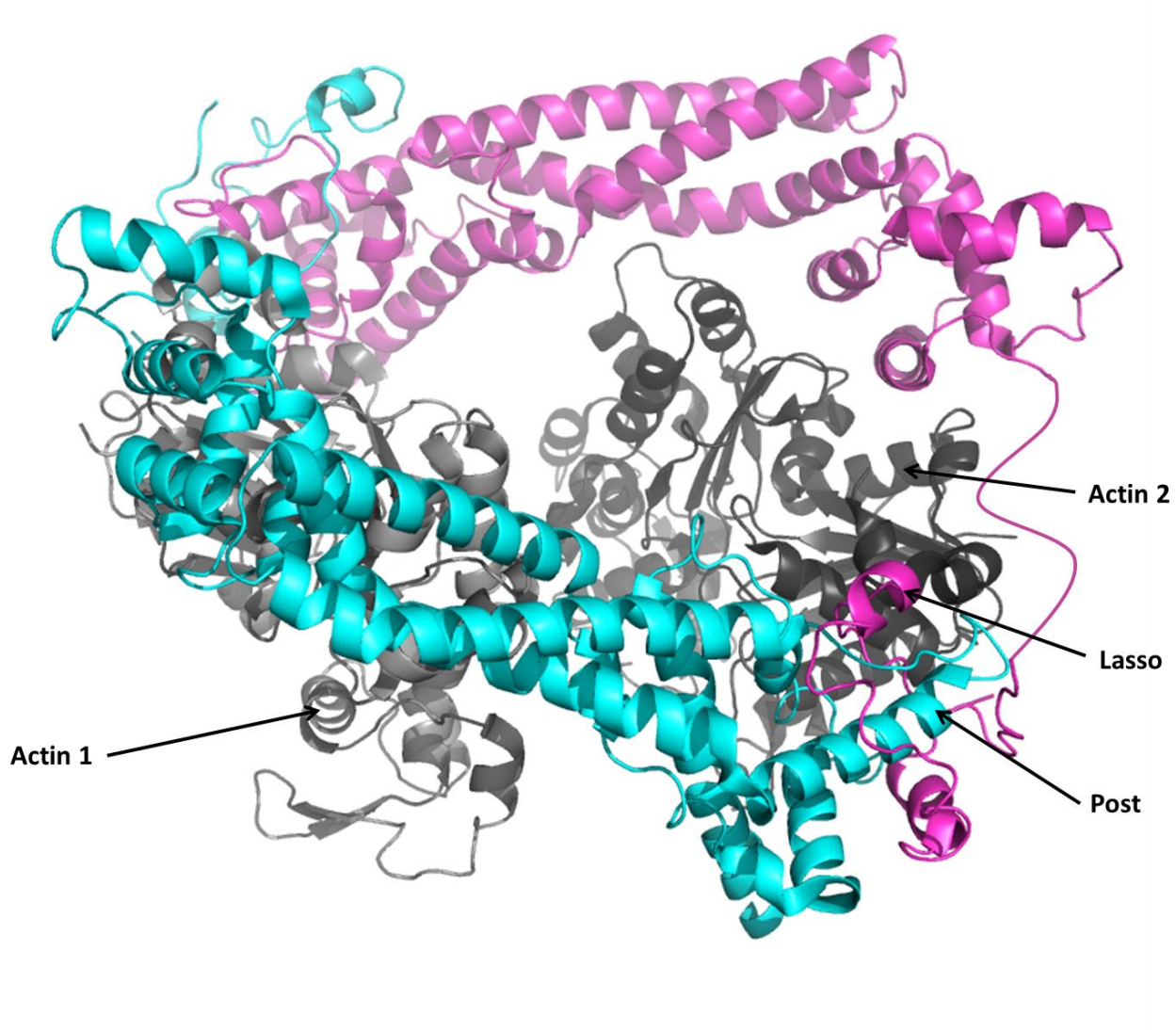

PDB: 4EAH

Figure 3. X-ray crystal structure of FH2 dimer from FMNL3 in complex with actin monomers. Purple and blue each represent one FH2 domain within the dimer. The lasso region at the N-terminus is able to interact with the post at the C-terminus of the next subunit to stabilize the dimer. The homodimer forms a donut structure which is able to surround an actin filament and remain attached.

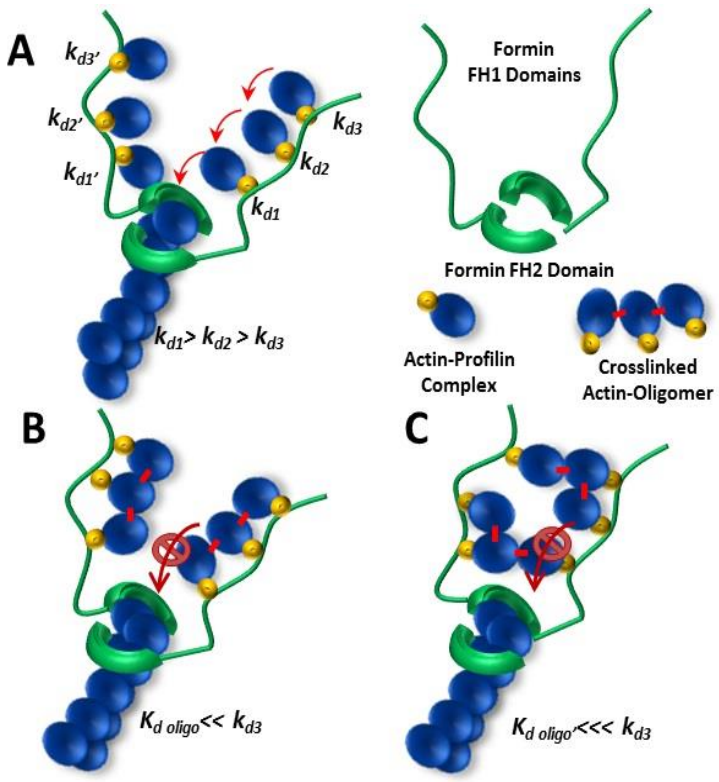

Figure 4. A) Accepted mechanism of formin-mediated actin polymerization in the presence of profilin. The poly-proline regions farthest from the filament have the strongest binding affinity for profilin-actin complexes while regions closer have weaker affinity and allow for quicker incorporation of these complexes into the filament. **B)** Our proposed mechanism for how profilin-bound actin oligomers block mDia1 mediated polymerization in the presence of profilin. **C)** An alternative proposed mechanism where actin oligomers are able to bind across FH1 arms, rather than along the tandem sites of a single FH1 arm.

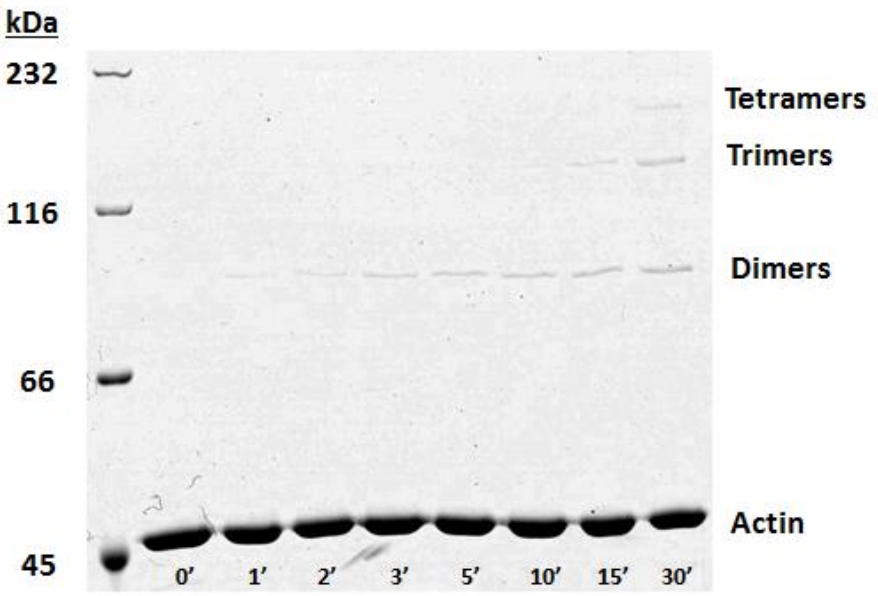

Figure 5. Time course of ACD activity in the presence of human profilin. Profilin concentration is 1.2x excess of actin concentration (10 uM), being crosslinked by 20 nM of ACD.

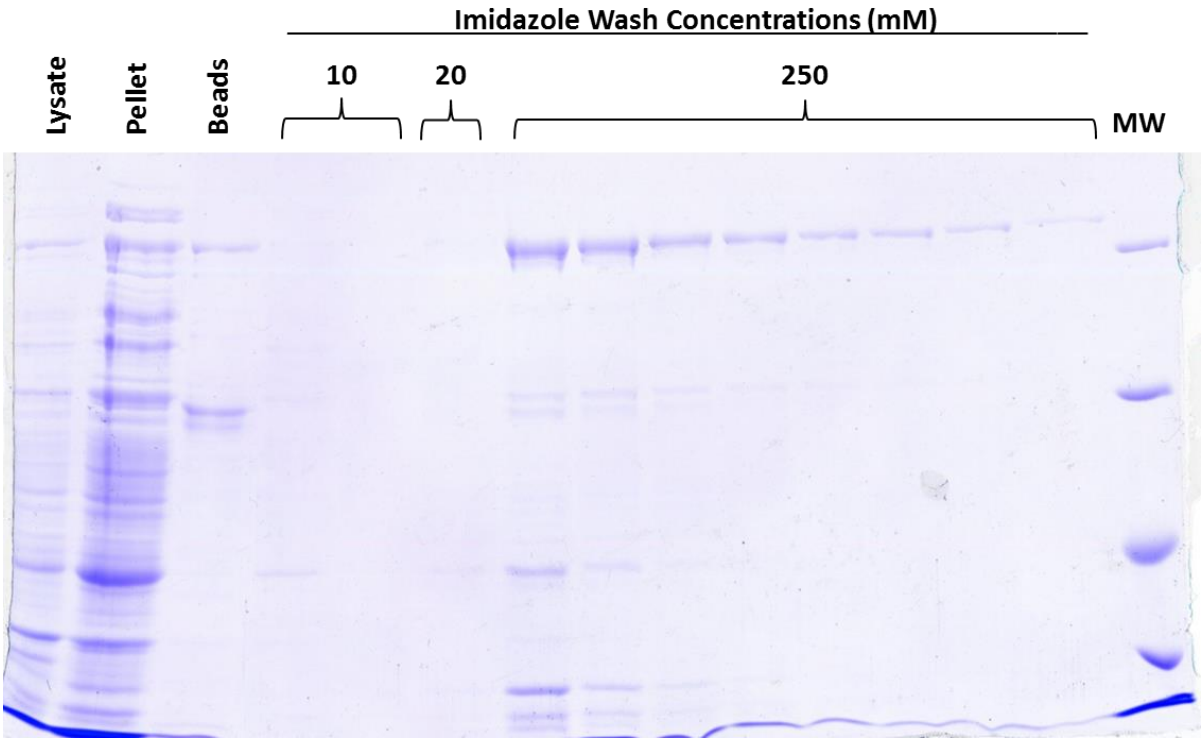

Figure 6. mDia1 purification SDS-PAGE. Lysate is shown after application and washing in the column. Washes represent increasing concentrations of imidazole for elution. Eluted contaminants cannot be visualized in 10 mM imidazole washes because they are significantly diluted in this step (50 mL total volume in each lane).

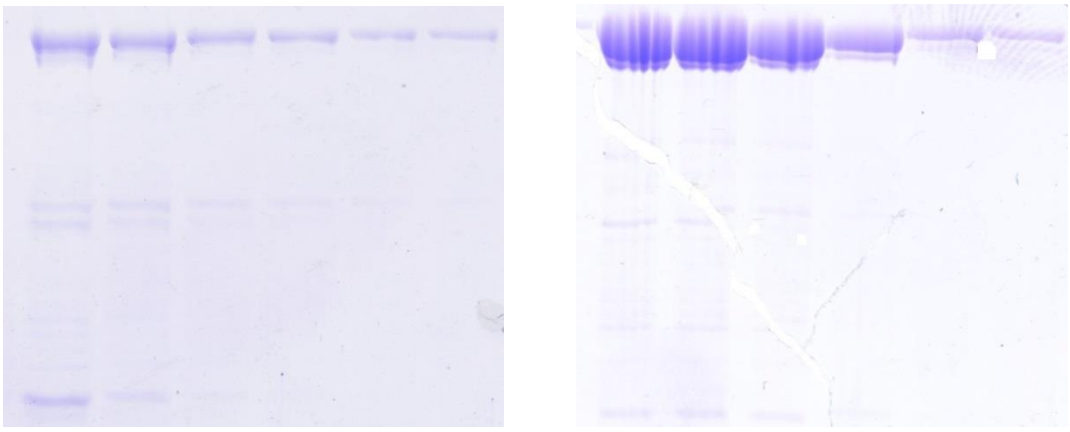

Figure 7. Yields of mDia1 before (left panel) and after (right panel) addition of free 0.5 M poly-L-proline. Panels show the first six elution fractions of protein in 250 mM imidazole.

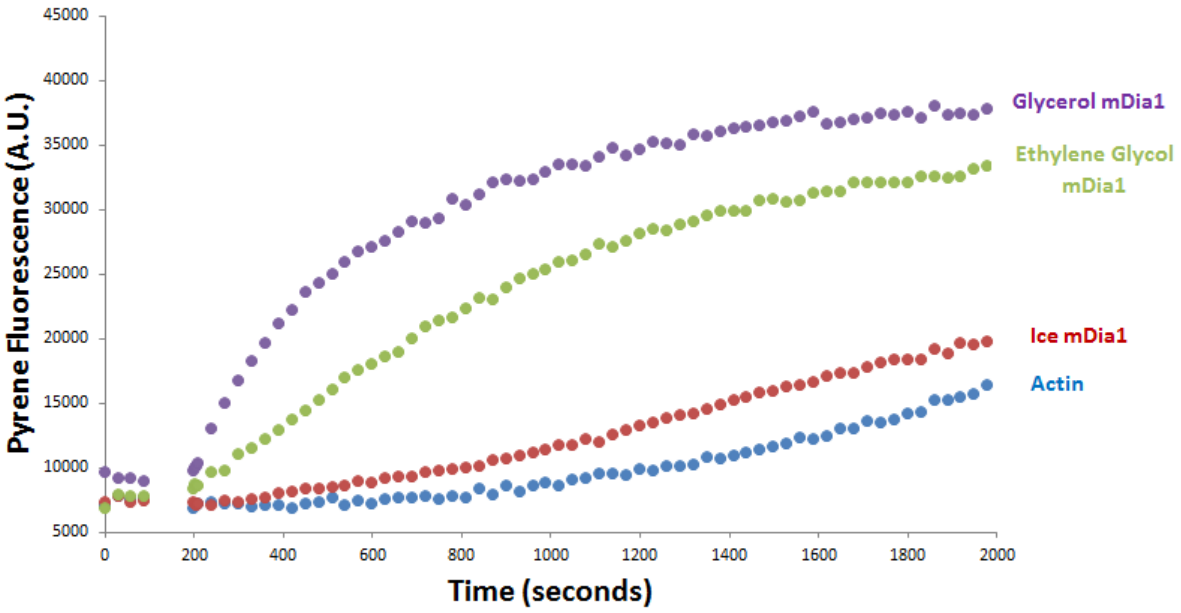

Figure 8. Comparison of storage methods for 2 week old mDia. 3 methods were used to attempt to preserve the protein: storage in 50% glycerol, storage in 50% ethylene glycol, and storage on ice. After 2 weeks, most significant activity loss was seen in mDia1 stored on ice.

Ethylene glycol stock activity was preserved much better than on ice, but not as well as the glycerol which was ultimately chosen as our storage method.

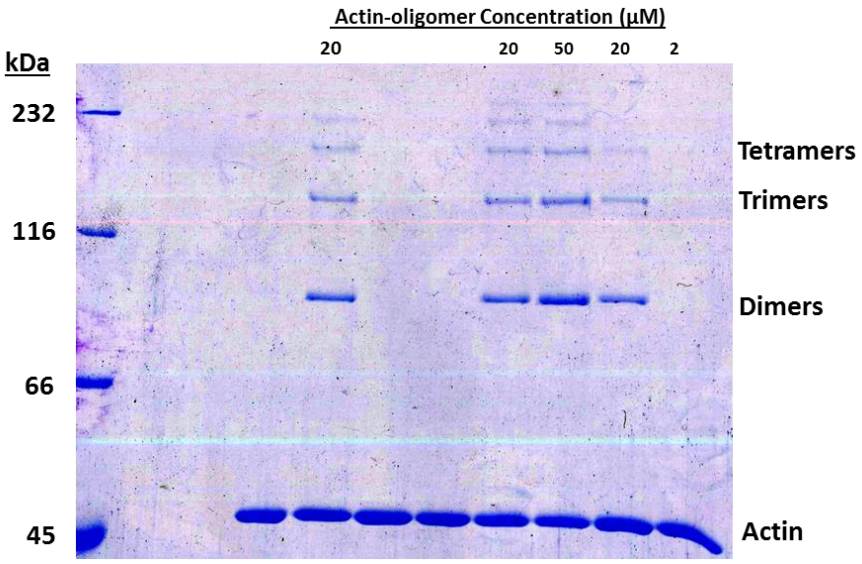

Figure 9. Example of ACD contamination being present in bulk-pyrene polymerization assays. Oligomers were added to the experiment in the nanomolar range, which should not be visualized by SDS-PAGE because the concentration is too low. Seeing actin oligomers by SDS-PAGE implies that additional monomeric actin was being crosslinked during the polymerization assay, meaning active ACD was still present. This can be affirmed by the slightly depleted monomeric actin bands at the bottom of the gel. All actin bands should be equal in size, but samples with large amounts of oligomers present also exhibit a depletion of the monomeric actin pool.

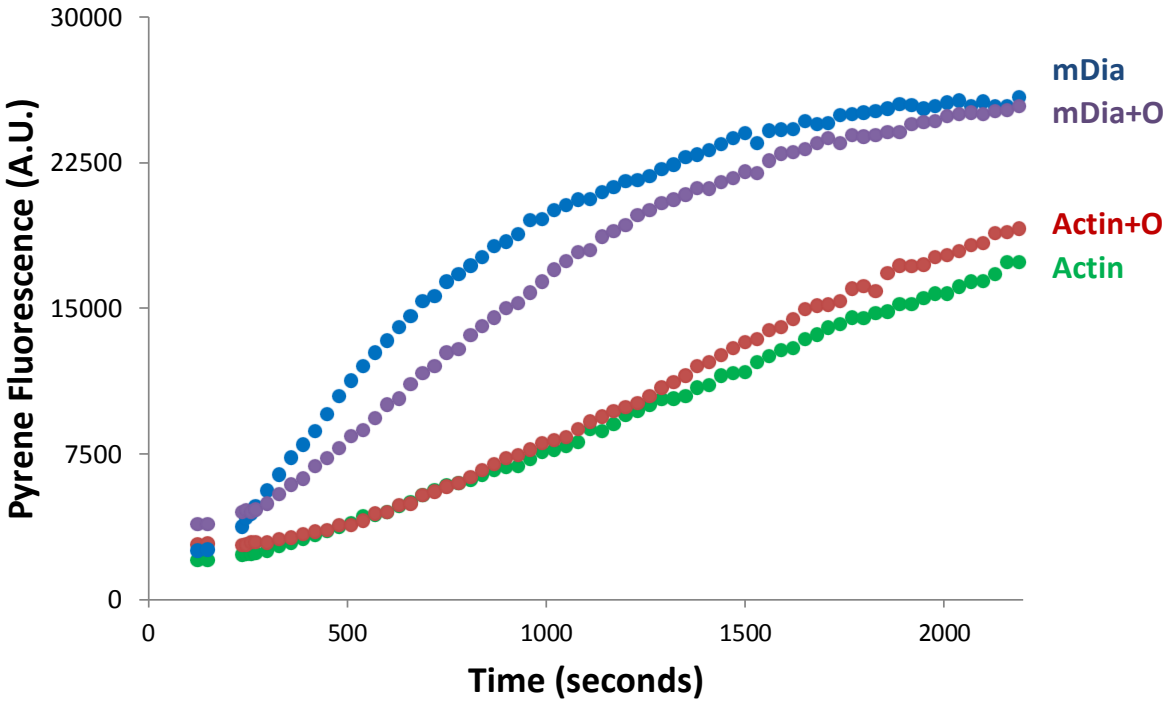

Figure 10. Control experiments to show the effects of actin oligomers on actin polymerization in the absence of profilin. Conditions used: 2.5 uM pyrene actin, 5 uM profilin, 5 nM mDia1. The green line represents the polymerization rate of actin alone, in the presence of 1 mM $MgCl_2$. Addition of actin oligomers does not significantly affect the polymerization rate. Blue represents the rate of mDia1 accelerated polymerization, and addition of actin oligomers (purple) also does not significantly inhibit this reaction. O=Oligomers.

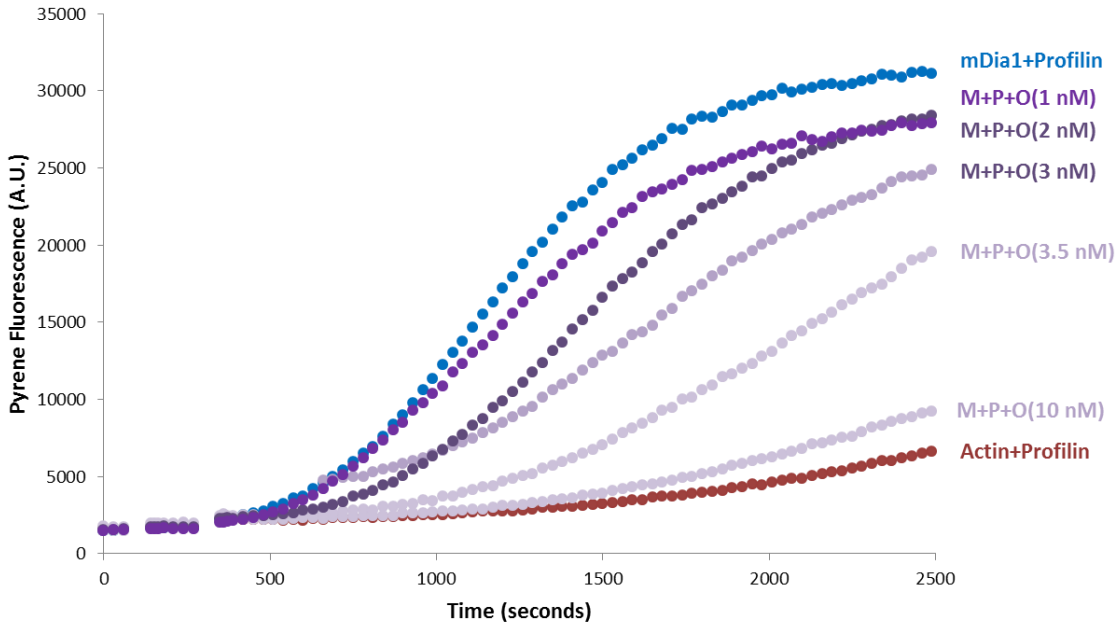

Figure 11. Observation of the effect of actin oligomers on mDia1 mediated polymerization in the presence of profilin. Conditions used: 2.5 uM pyrene actin, 5 uM profilin, 5 nM mDia1. Profilin is shown to function properly as it sequesters actin monomers and slows polymerization on its own (red line). mDia1 in the presence of profilin shows the greatest rate of polymerization (blue line), and is then inhibited in a stepwise fashion as increasing concentrations of actin oligomers (purple lines) are titrated into the system. M=mDia1, P=hProfilin, O=Oligomers with their concentration at that specific point added in parentheses.

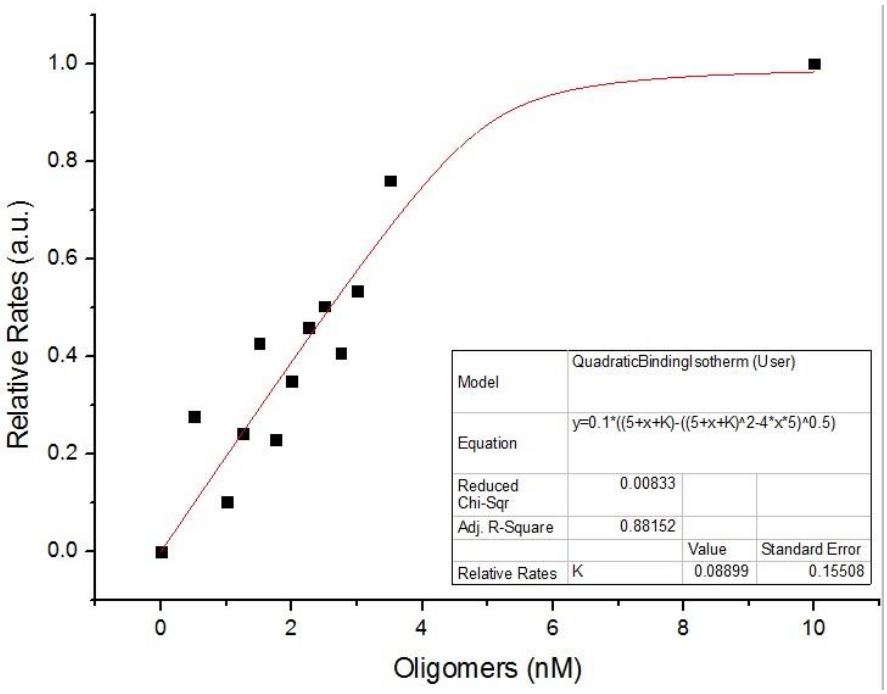

Figure 12. Isothermal binding curve calculated using sub-stochiometric concentrations of actin oligomers, relative to the concentration of mDia1. The calculated affinity value from this curve is 0.089 nM, suggesting a very strong interaction between profilin bound actin oligomers and the FH1 domain. This curve gives an apparent K_D because we study a mixed population of actin oligomers as opposed to a homogenous population.

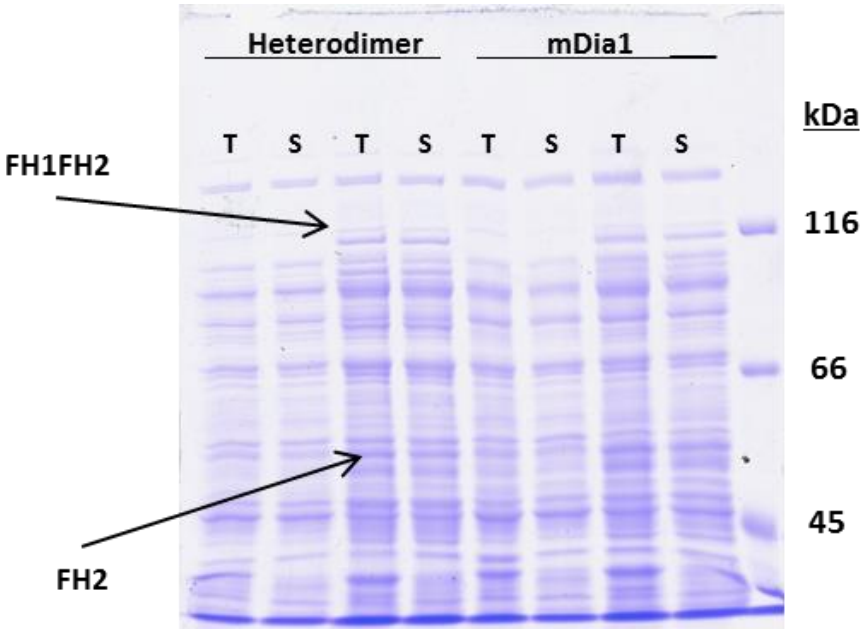

Figure 13. SDS-PAGE showing heterodimer expression at 37 C, compared to mDia1 expression. First two lanes for heterodimer show total and supernatant of unexpressed cells versus the next two lanes which show total and supernatant after expression. Bands corresponding in size to FH1FH2 and FH2 are shown on the gel by arrows.

References

Breitsprecher, D., and Goode, B.L. (2013). Formins at a glance. J. Cell Sci. *126*, 1–7.

Bugyi, B., and Carlier, M.-F. (2010). Control of actin filament treadmilling in cell motility. Annu. Rev. Biophys. *39*, 449–470.

Cooper, J. a, Walker, S.B., and Pollard, T.D. (1983). Pyrene actin: documentation of the validity of a sensitive assay for actin polymerization. J. Muscle Res. Cell Motil. *4*, 253–262.

Cordero, C.L., Kudryashov, D.S., Reisler, E., and Satchell, K.J.F. (2006). The Actin cross-linking domain of the Vibrio cholerae RTX toxin directly catalyzes the covalent cross-linking of actin. J. Biol. Chem. *281*, 32366–32374.

Courtemanche, N., and Pollard, T.D. (2012). Determinants of Formin Homology 1 (FH1) domain function in actin filament elongation by formins. J. Biol. Chem. *287*, 7812–7820.

Dominguez, R., and Holmes, K.C. (2011). Actin structure and function. Annu. Rev. Biophys. *40*, 169–186.

Gasteiger, E., Hoogland, C., Gattiker, A., Duvaud, S., Wilkins, M.R., Appel, R.D., and Bairoch, A. Protein Identification and Analysis Tools on the ExPASy Server. 571–608.

Irwin, C.R., Farmer, A., Willer, D.O., and Evans, D.H. (2012). Vaccinia Virus and Poxvirology. *890*, 23–35.

Kudryashov, D.S., Cordero, C.L., Reisler, E., and Satchell, K.J.F. (2008a). Characterization of the enzymatic activity of the actin cross-linking domain from the Vibrio cholerae MARTX Vc toxin. J. Biol. Chem. *283*, 445–452.

Kudryashov, D.S., Durer, Z. a O., Ytterberg, a J., Sawaya, M.R., Pashkov, I., Prochazkova, K., Yeates, T.O., Loo, R.R.O., Loo, J. a, Satchell, K.J.F., et al. (2008b). Connecting actin monomers by iso-peptide bond is a toxicity mechanism of the Vibrio cholerae MARTX toxin. Proc. Natl. Acad. Sci. U. S. A. *105*, 18537–18542.

Moseley, J.B., Maiti, S., and Goode, B.L. (2006). Formin proteins: purification and measurement of effects on actin assembly. Methods Enzymol. *406*, 215–234.

Netea, M.G., van de Veerdonk, F.L., and van der Meer, J.W.M. (2012). Primary immunodeficiencies of pattern recognition receptors. J. Intern. Med. *272*, 517–527.

Park, S., and Raines, R.T. to Quantify Protein – Protein Interactions. *261*, 161–165.

Paul, A.S., and Pollard, T.D. (2009). Review of the mechanism of processive actin filament elongation by formins. Cell Motil. Cytoskeleton *66*, 606–617.

Pollard, T.D., and Cooper, J. a (2009). Actin, a central player in cell shape and movement. Science *326*, 1208–1212.

Satchell, K.J.F. (2009). Actin Crosslinking Toxins of Gram-Negative Bacteria. Toxins (Basel). *1*, 123–133.

Schoenenberger, C.A., Mannherz, H.G., and Jockusch, B.M. (2011). Actin: From structural plasticity to functional diversity. Eur. J. Cell Biol. *90*, 797–804.